Latin American Journal of Solids and Structures
www.lajss.org

Parameters Determination of Yoshida Uemori Model Through Optimization Process of Cyclic Tension-Compression Test and V-Bending Springback

Abstract

In recent years, the studies on the enhancement of the prediction capability of the sheet metal forming simulations have increased remarkably. Among the used models in the finite element simulations, the yield criteria and hardening models have a great importance for the prediction of the formability and springback. The required model parameters are determined by using the several test results, i.e. tensile, compression, biaxial stretching tests (bulge test) and cyclic tests (tension-compression). In this study, the Yoshida-Uemori (combined isotropic and kinematic) hardening model is used to determine the performance of the springback prediction. The model parameters are determined by the optimization processes of the cyclic test by finite element simulations. However, in the study besides the cyclic tests, the model parameters are also evaluated by the optimization process of both cyclic and V-die bending simulations. The springback angle predictions with the model parameters obtained by the optimization of both cyclic and V-die bending simulations are found to mimic the experimental results in a better way than those obtained from only cyclic tests. However, the cyclic simulation results are found to be close enough to the experimental results.

Keywords

Springback, Yoshida Uemori model, Optimization, 5XXX Aluminum

Serkan Toros [a, b]

[a] Nigde University, Mechanical Engineering Department, Nigde 51240, Turkey,

[b] Nigde University Prof. Dr. T. Nejat Veziroglu Clean Energy Research Center, 51245, Nigde, Turkey

Author email: serkantoros@nigde.edu.tr

http://dx.doi.org/10.1590/1679-78252916

Received 16.03.2016
In revised form 12.04.2016
Accepted 20.04.2016
Available online 21.04.2016

1 INTRODUCTION

It is quite well known fact that the material and process parameters as the inputs to the finite element analysis (FEA) program have a considerable influence on the accuracy of the results. Since

sheet materials have anisotropic behaviors due to the rolling operation and crystal structures, the use of anisotropic yield functions in the simulations increases the accuracy of the prediction. In addition to the used anisotropic yield criterion functions, the hardening model parameters (i.e. isotropic, kinematic and combined isotropic-kinematic hardening) are also important effective parameters for the accuracy of the simulation results. Particularly, the kinematic and combined isotropic-kinematic hardening models are important for the forming simulation of the most of aluminum alloys as well as advanced high strength steels (TRIP "Transformation Induced Plasticity", TWIP "Twining Induced Plasticity", and DP "Dual Phase" steels) which have a high tendency to springback due to the relatively high yield strength they show. Recently, the prediction of the formability and springback characteristics of these materials have been shown to be enhanced by using the cyclic plasticity models in which the different deformation combinations like tension-compression are well defined (Uemori et al., 1998, 2000). In the real stamping operations of sheet metals, some specific regions are generally exposed to different deformation path during the flowing through the die cavity. The main problem in a classical modelling (isotropic) approach is the assumption of the same mechanical responses under different loading conditions. However, most of the sheet materials behavior under forward and reverse loading directions is not the same and the difference between these loading conditions is called as Bauschinger effect. The Bauschinger effect is mainly addressed to the early yielding of the metals when the loading direction is reversed.

The contribution of the Bauschinger effect on the springback characterization of materials was firstly modelled by Prager (Prager, 1956) and then this model was modified by Ziegler (Zeigler, 1959). These models only consider the kinematic part of the hardening mechanism in which the shape of the yield surface is kept constant, but the central positon is movable with the given deformation. In most cases, since the transient behavior of the materials does not obey this linear hardening mechanism, a nonlinear kinematic hardening rule was proposed by Armstrong and Frederick (Frederick and Armstrong, 2007). Then, Chaboche (Chaboche, 1986, 1989) proposed the modified Armstrong and Frederick non-linear kinematic hardening model to improve the prediction capability of the model for transient behavior. This model can be also considered to be the most commonly used hardening model in finite element simulations. These models are then modified or re-modelled by several researchers to increase the representability of material behavior (Choi et al., 2006a, b; Chun et al., 2002a; Chun et al., 2002b). Besides, these linear and non-linear kinematic hardening models, another most important hardening models is the combined isotropic-kinematic hardening models with two surface plasticity models. In these models, the small yield surface describes the kinematic part of the hardening and the bound surface represents the isotropic part of the hardening characterization. Two surface plasticity model was first described by Dafalias and Popov (Dafalias and Popov, 1975). Since the representation capability of these models is higher than the other models which contain only the isotropic or kinematic form of the hardening behavior, many researchers has started to improve these two surface plasticity models with a well described permanent softening obtained after the reverse loading conditions (McDowell, 1985a, b; Mroz, 1967; Tseng and Lee, 1983; Yoshida and Uemori, 2002). One of the most famous two surface plasticity models is the Yoshida-Uemori (Y-U) (Yoshida and Uemori, 2002) model which has been frequently implemented to finite element software. One of the main advantage of this two surface plasticity

model is that it can be used with any anisotropic yield criteria. Moreover, it allows defining of elasticity modulus as variable with the given deformation.

Despite the high accuracy of the Y-U model for the prediction of springback, some special experiments are required to determine the model parameters. In literature, there are several experimental and numerical procedures to obtain the cyclic loading behavior of the materials. One of the most commonly used cyclic test is the tensile-compression test (Boger et al., 2005; Kim et al., 2013; Lee et al., 2005a; Yoshida et al., 2002) in which the special geometric sheets are compressed between lubricated plates to prevent buckling. However, this experiment is not satisfactory because of the buckling problem in case of large strain levels are aimed. The other experimental method for the determination of the model parameters is the shear type cyclic deformation. In the experiments, generally "*H*" type geometric samples are used to obtain the hysteresis stress-strain curves (Kim et al., 2013; Zang et al., 2011). In order to measure the deformations on the narrow shear regions, a specific non-contact deformation measurement system Aramis-GOM (Yin et al., 2012) is required since it has the capability of measuring of the whole active deformation region. It is also possible to measure the shear deformations in the active region by calculating the actual positions of the marked points on the sample via a video type camera as suggested in Thuillier and Manach's study (Thuillier and Manach, 2009). Another experimental method used for obtaining the cyclic loading condition is the three point bending test by which the reverse loading condition can also be considered. Unfortunately, it is not possible to provide the stress strain hysteresis loop with this experiment directly. Some additional calculations are essential to convert the measured forces and displacements of the sheet metals to stress-strain data analytically (Hiroshi Hamasaki et al., 2011; Lee et al., 2005b). Zang et al. (Zang et al., 2011) proposed a novel approach to determine the nonlinear kinematic hardening model parameters via the optimization of the three point bended specimens which are pre-strained. In addition, U-Bending test and shear type cyclic test of a dual phase steel are also carried out to validate the new approach. According to the study, springback predictions are found to be good agreement with the determined model parameters by the classic shear type cyclic test optimization. Furthermore, definition of the elasticity modulus as variable with the given deformation shows the increasing the springback prediction performance.

As aforementioned before, these hardening models were mostly developed to enhance the prediction capability of finite element simulation of the springback behavior of materials. In the current study, on the other hand, the parameters of Y-U model are determined by the optimization of the model with the obtained stress-strain curve from tensile and compression tests. Additionally, the optimization procedure is improved by adding a springback target that is obtained by V-Die bending test since the simulation results are generally not satisfactory for several cases and different materials.

2 EXPERIMENTAL WORK OF TENSION-COMPRESSION, V-DIE BENDING AND U-BENDING TEST

2.1 Tension-Compression Test

In order to obtain a cyclic stress-strain curve, a tension-compression test setup was manufactured and adapted to the computer controlled SHIMADZU-Autograph 100kN tensile testing machine.

The given strain levels were controlled by a specific software in which any kind of linear deformation can be detected. In order to measure the strains on the specimens via the video type extensometer, sandwich plates were manufactured from the Plexiglas materials plate which are shown in figure 1. The lines (gauge marks) on the specimens can be followed by the used computer program. In order to reduce friction, mineral oil is used between the sample and plates. Additionally, since the roughness of the plates are very low, easy sliding of the samples between the plates is achieved.

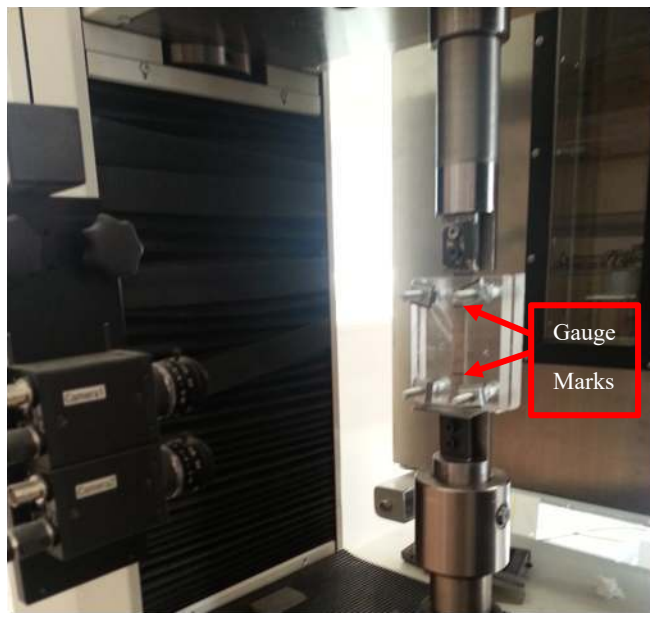


Figure 1: Experimental setup of the tension-compression test.

Tensile tests were performed to determine the mechanical properties of materials which were prepared according to the ASTM-E8 standard as shown in figure 2. These tests were also performed by the SHIMADZU-Autograph 100kN tensile testing machine. The calculated Lankford parameters from the tests were used in Hill-48 (Hill, 1948) anisotropic yield function.

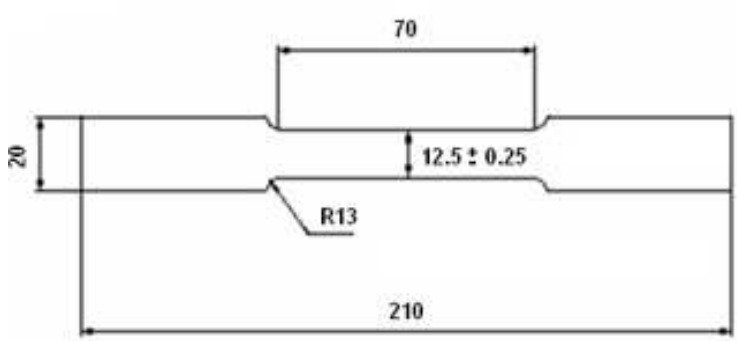


Figure 2: Tensile test specimen geometry (all dimensions are in mm).

2.2 60° V-Shaped Die Bending

In the study, an experiment was carried via a 60° V shape die to determine the springback tendency of the sheet materials. The geometric features of the tools are illustrated in figure 3 and the distance between the shoulders of the die is 100 mm. The rolling direction of bending specimen is also shown in the figure. The samples were cut into 200 mm length and 35 mm wide. The bending process was carried out under a specific punch speed of 25mm/min for three different samples in the rolling direction. The tools were adopted to the tensile test machine to control the punch travel and coining force. After applying deformation, the springback angle was measured by the Mitutoyo 187-907 universal bevel protractor with the minimum angle reading accuracy of 5 min. The obtained springback angle result was then used as a target value for the springback optimization.

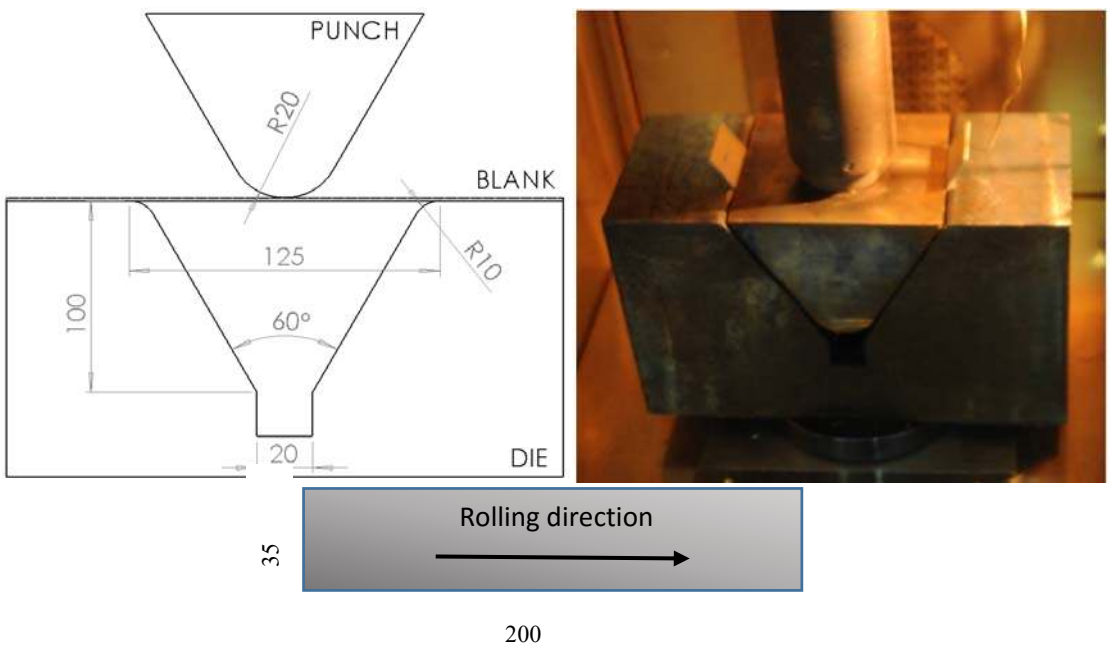


Figure 3: 60° V-shaped bending test setup (all dimensions are in mm).

2.3 U-Bending Test

Besides the V-die bending test, U-bending tests were also performed in samples to validate the model parameter determination approach. Figure 4 depicts the experimental setup of the U-bending test system which was adopted to tensile test devise. The rolling direction of bending specimen is also shown in the figure. The samples which have the same dimensions in V-die bending tests were tested at 25 mm/min deformation speeds and the springback behavior of the samples were measured via the same measurement system. In addition, the punch was manufactured as modifiable since the materials have various thicknesses. The sides of the punch can be changed according to sheet thickness.

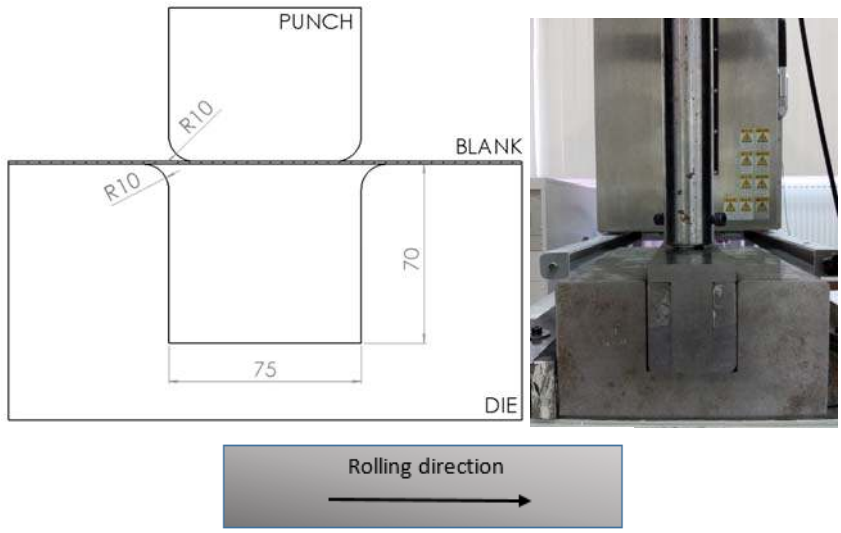


Figure 4: Experimental setup of U-Bending Test System.

3 OPTIMIZATION PROCESS OF TENSION-COMPRESSION TEST AND 60^{O} V-SHAPED DIE BENDING TEST

3.1 Yoshida-Uemori Model

The Y-U model has two surface plasticity features for modeling the kinematic move of the yield contour within a bounding surface. The main advantage of this model is that it is a powerful tool for evaluating the Bauschinger effect and the work hardening stagnation with the given reverse deformations. Since it is able to describe the cyclic stress-strain relation in a better way, the model is implemented in many commercially available finite element simulation software like LsDyna and Pam-Stamp. The high capability of the model for the prediction of the springback of materials was proven by many researchers (Alghtani et al., 2013; Aryanpour and Green; Kessler et al., 2008). The schematic illustration of the two moving surface plasticity model is given in figure 5.

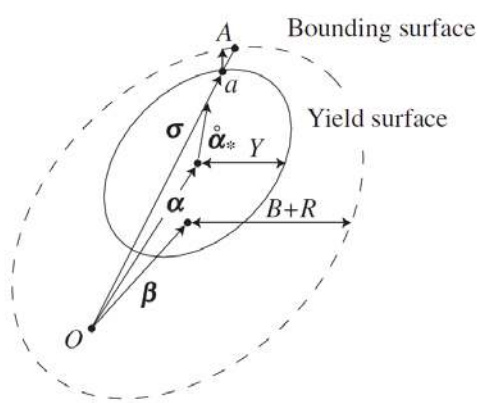


Figure 5: Schematic illustration of the two moving surface Y-U model.

In the model, the initial form of the yielding surface or yield function can be modeled by the following equation:

$$f_0 = \varphi(\boldsymbol{\sigma}) - Y = 0 \tag{1}$$

where $\varphi(\boldsymbol{\sigma})$ denotes the selected anisotropic yield criterion, $\boldsymbol{\sigma}$ is the Cauchy stress tensor and Y is the initial yield strength of the materials. In the Y-U model, the most commonly used quadratic Hill-48 anisotropic yield criterion is chosen for the yield contour of the materials. Under reverse loading conditions, the materials may show the distinctive early yielding and in this case, the yield contour is assumed to be kinematic hardening while the bounding surface is combined hardening behavior. For the subsequent deformation of the materials, the yield function for kinematic hardening can be defined as:

$$f_0 = \varphi(\boldsymbol{\sigma} - \boldsymbol{\alpha}) - Y = 0 \tag{2}$$

where $\boldsymbol{\alpha}$ stands for the backstress which varies with the applied effective plastic strain rate. The bounding surface F can be expressed with an additional parameter that shows the center of the bounding surface $\boldsymbol{\beta}$ as:

$$F = \varphi(\boldsymbol{\sigma} - \boldsymbol{\beta}) - (B + R) = 0 \tag{3}$$

where the B and R are the initial size and isotropic hardening component of the bounding surface and $B+R$ represents the size of the bounding surface. The kinematic motion of the yield surface with respect to the bounding surface is expressed by the following relation:

$$\boldsymbol{\alpha}_* = \boldsymbol{\alpha} - \boldsymbol{\beta} \tag{4}$$

The $\boldsymbol{\alpha}$ and $\boldsymbol{\beta}$ can be expressed as follows**:**

$$\boldsymbol{\alpha} = \begin{pmatrix} \alpha_{11} \\ \alpha_{22} \\ \alpha_{12} \end{pmatrix}; \quad \boldsymbol{\beta} = \begin{pmatrix} \beta_{11} \\ \beta_{22} \\ \beta_{12} \end{pmatrix} \tag{5}$$

$$\dot{\alpha}_* = C\left[\left(\frac{a}{Y}\right)(\boldsymbol{\sigma} - \boldsymbol{\alpha}) - \sqrt{\frac{a}{\overline{\boldsymbol{\alpha}}_*}}\boldsymbol{\alpha}_*\right]\dot{\bar{\varepsilon}} \tag{6}$$

where $\overline{\boldsymbol{\alpha}}_*$ is the equivalent form of the kinematic motion of the yield surface with respect to the bounding surface ($\overline{\boldsymbol{\alpha}}_* = \varphi(\boldsymbol{\alpha}_*)$) while a can be found via the following equation:

$$a = B + R - Y \tag{7}$$

In Equation (7), Y is the size of the yield surface and is constant throughout the deformation process. The equivalent strain rate is given as follows:

$$\dot{\bar{\varepsilon}} = \sqrt{\frac{2}{3}\dot{\boldsymbol{\varepsilon}}^{\boldsymbol{p}} : \dot{\boldsymbol{\varepsilon}}^{\boldsymbol{p}}} \tag{8}$$

The tentative prediction in size and center of the bounding surface can be defined as:

$$\dot{R} = k(R_{sat} - R)\dot{\bar{\varepsilon}} \tag{9}$$

$$\dot{\beta}_* = m\left[\left(\frac{b}{B+R}\right)(\boldsymbol{\sigma} - \boldsymbol{\beta}) - \boldsymbol{\beta}\right]\dot{\bar{\varepsilon}} \tag{10}$$

In addition to the calculation of the yield surfaces, the definition of the elasticity modulus variation is an important feature of the model and this variation is defined by the following equation:

$$E = E_0 - (E_0 - E_A)(1 - \exp(-\xi\bar{\varepsilon})) \tag{11}$$

where E_0 is the initial elasticity modulus of the materials and E_A is the minimum value at the end of given plastic deformation. ξ, on the other hand, is the decreasing rate of the elasticity modulus with the given deformation, $\bar{\varepsilon}$. The decrease in the elasticity modulus of the materials is generally determined via the loading and unloading tests applied to tensile test specimens. The tendency of the stress strain data obtained during the unloading and reloading situations is used to calculate the variation of the elasticity modulus. However, it is also possible to determine indirectly this variation with the optimization process. Therefore, the Y-U model can be defined by 9 parameters (Y, B, C, $Rsat$, k, b, m, E_A, *and* ξ) that reflect the material behavior.

3.2 60° V-Die Bending and U Bending Simulations

The finite element simulations of bending processes were carried out under the plane strain condition by a commercially available Ls-DYNA software. The views of the generated models were displayed in figure 6 schematically. In the simulations, the Y-U model was selected for the calibration of model parameters according to the springback prediction results of 60^o V die bending process and finally the obtained model parameters were used in the U-bending simulations to validation of the model parameter determination approach. The Coulomb friction coefficient between the blank and dies was assumed to be constant and it was taken as 0.15 for the aluminum alloys. In addition, Belytschko-TSAY shell element was used for the blank and rigid tools. The adaptive mesh feature of the software was performed to the work piece during the simulation in order to overcome the convergence problems, large element distortion and increase the accuracy of the simulations.

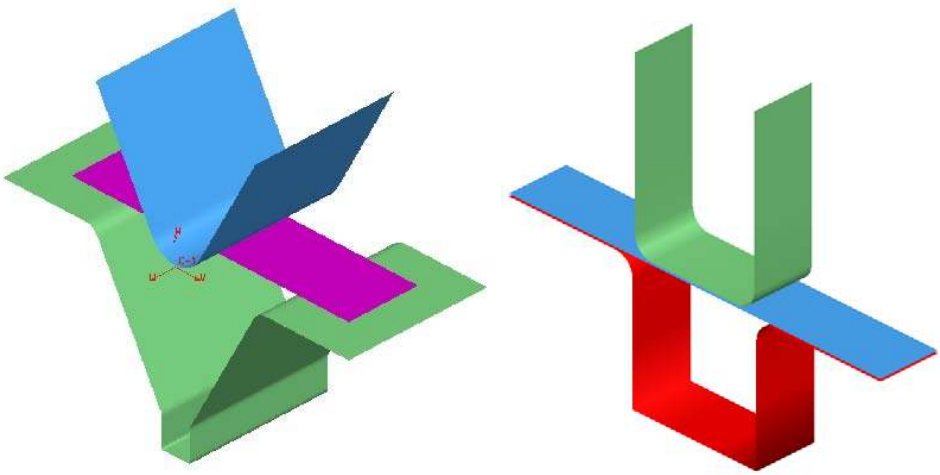


Figure 6: 60° V-shaped die and U bending simulations.

Similar to V-die bending simulation, the designed experimental setup for the tension-compression test was also simulated to determine Y-U model parameters. In these simulations, specified strain levels were applied to the selected unit element while the stresses/strains on the unit element are recorded and compared with the experimental cyclic results during the optimizations.

3.3 Optimization Process of the Stress-Strain Cycle and Springback

The determined model parameters with respect to the obtained tension-compression test results may give a reasonable springback prediction as proven in the literature. It is well known in literature, in sheet metal forming of aluminum alloys exhibiting the coefficient of anisotropy r lower than 1, that Hill 48 yield criterion has poor correlation with experimental yield curve results. The poor prediction capability of Hill 48 can be improved by embedding the error in the Y-U model parameters. Beside the tension-compression test simulations, 60° V-die bending simulation was also adopted to the optimization processes in order to increase the springback prediction capability of the model by modifying the values of the model parameters. It was aimed to determine more appropriate model parameters that would predict the springback of the specimens more accurately. In order to achieve that, 60° V-die bending model was established in the commercially available Ls-DYNA software and a **.k* file was generated. In this generated file, the model parameters (Y, B, C, $Rsat$, k, b, m, E_A, and ξ) were defined as design parameters. After the required modifications were performed to the file, it was imported to the Ls-OPT V.5. In the optimization procedure, sequential response surface method (SRSM) (Stander and Craig, 2002) was used as a metamodel-based optimization to determine an approximate optimum point for the design variables. Additionally, the polynomial surface response was used to determine the significance of the parameters and the interactions between the each other was constructed. A general scheme of the model parameter identification procedure is also given in figure 7. As can be seen from the scheme, the response of the cyclic and V-die bending simulations were evaluated together and if a reasonable error was not obtained for the selected parameter values, the initial parameters would be modified again.

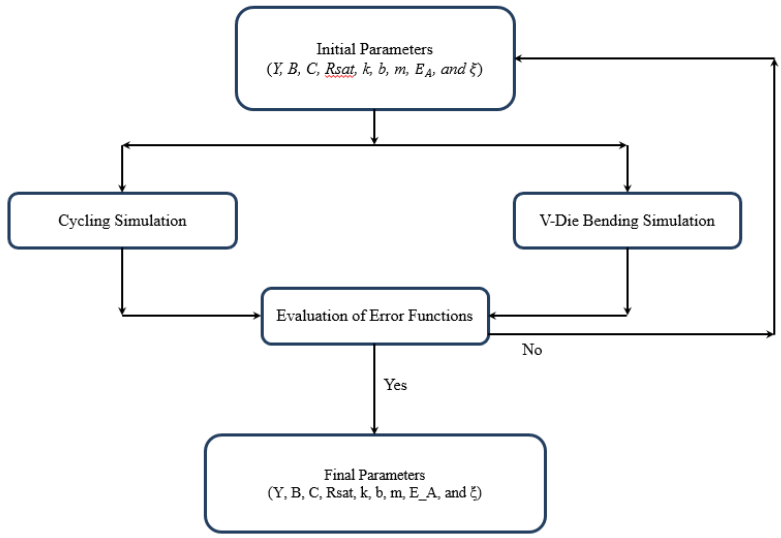


Figure 7: Scheme of the material parameter identification procedure.

In the study, the springback results of 60° V-die bending simulation were calculated by determining the selected node coordinates recorded in the history file. Since the springback decides the final shape of the geometry, the responses of the simulations for the prescribed nodes were considered. The coordinates of the selected nodes at the final stage of the simulations were used in Eq.12 to calculate the final angle between the two arms of the bended sheet specimen. In the equation, the $\boldsymbol{Z_i}$ and $\boldsymbol{Y_i}$ (i=1...4) are the coordinates of the selected nodes in z and y directions, respectively. The description of the calculations was depicted in figure 8. In Eq. 13, the target function that needs to be minimized during the simulations was given. The $\theta_{simulation}$ was obtained from the final angle between the arms as following:

$$\theta_{simulation} = 180 - (-\text{atan}\left(\frac{Z_3 - Z_4}{Y_3 - Y_4}\right) + \text{atan}\left(\frac{Z_1 - Z_2}{Y_1 - Y_2}\right)) \tag{12}$$

$$f_{target} = \theta_{simulation} - \theta_{experiment} \tag{13}$$

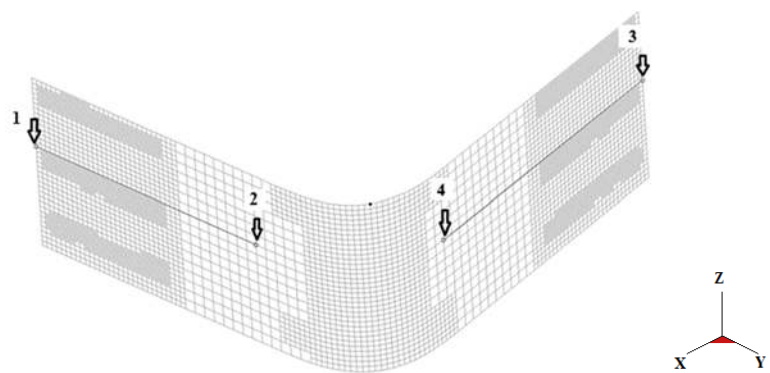


Figure 8: Mesh and calculation method of the springback angle.

4 RESULTS AND DISCUSSION

The tensile tests were performed to the specimens which were prepared at different directions by the water jet cutting process to determine the mechanical properties like yield strength and Lankford parameters. The tensile tests were performed at 25 mm/min (0.0083 s^{-1}) deformation speed. 5754-H22, 5083-O and 5005-O aluminum alloys were selected as a target material which have been started to use in automotive components frequently to reduce the weight of the structures without sacrificing the strength. The determined mechanical properties were used in the anisotropic yield function Hill-48. The yield strengths and Lankford parameters were tabulated in Table 1. Additionally, the strain hardening curve was represented by the Hollomon Equation and the strength coefficient (K), the strain hardening exponent (n) and finally the initial yield strain value (ε_o) were determined for the rolling direction and listed in the Table 1. The thickness of the selected materials were 0.97 mm for 5754-H22 and 2 mm for both 5083-O and 5005-O. The true stress strain curves of the sample for different orientations are compared in figure 9. As can be seen from the figures, the hardening curves of the studied aluminum alloys depict the scattering in the plastic deformation region. These behavior is known as Luder's band and it is related with the solute atoms in the microstructure. The main alloying element of these 5XXX series aluminum alloys is magnesium which behaves as an obstacle for the dislocations. During the moving of dislocations with given deformation, they are pinned and the required force increases locally. Unfortunately, these stretching strain marks create trouble during the painting operation of the components. In literature, there exist several methods suggested to eliminate this problem by increasing the forming temperature and strain rate (Ozturk et al., 2009).

As can be seen from the given information in Table 1, although the yield strength of the materials are close to each other, the hardening coefficients which shows the formability are very different. 5083-O aluminum alloy was found to have the highest formability among the studied materials. In addition to tensile tests, the variation of the elasticity modulus with the plastic deformation was determined by performing the loading-unloading tests. Figure 10 and 11 show the obtained stress-strain curves at rolling direction and the variation of the elastic modulus with their best fit for Eq.(11), respectively. It is seen that, the elastic modulus of the studied aluminum alloys decreases with the given plastic deformation. Since the 5754-H22 aluminum alloy contains the rolling operation effects, its elastic modulus has the lowest value compared to the other materials. The fitting parameters belonging to the specimens at rolling direction of the Eq. (11) were given in Table 2. The tests were carried at 1 mm/min to reduce the machine compliance errors. Therefore, the stretcher strain marks are more distinctive than those under the 25 mm/min deformation speeds.

Materials	Thickness (mm)	$\boldsymbol{\sigma_0}$	$\boldsymbol{\sigma_{45}}$	$\boldsymbol{\sigma_{90}}$	$\boldsymbol{\varepsilon_0}$	K	n	$\mathbf{r_0}$	$\mathbf{r_{45}}$	$\mathbf{r_{90}}$
5754-H22	0.97	141.25	143.24	141.77	0.0022	425	0.20	0.50	0.66	0.61
5083-O	2	142.85	139.24	142.84	0.0036	594	0.29	0.53	0.79	0.50
5005-O	2	141.01	132.73	144.84	0.0028	310	0.14	0.46	0.76	0.69

Table 1: Summary of measured and calculated material properties.

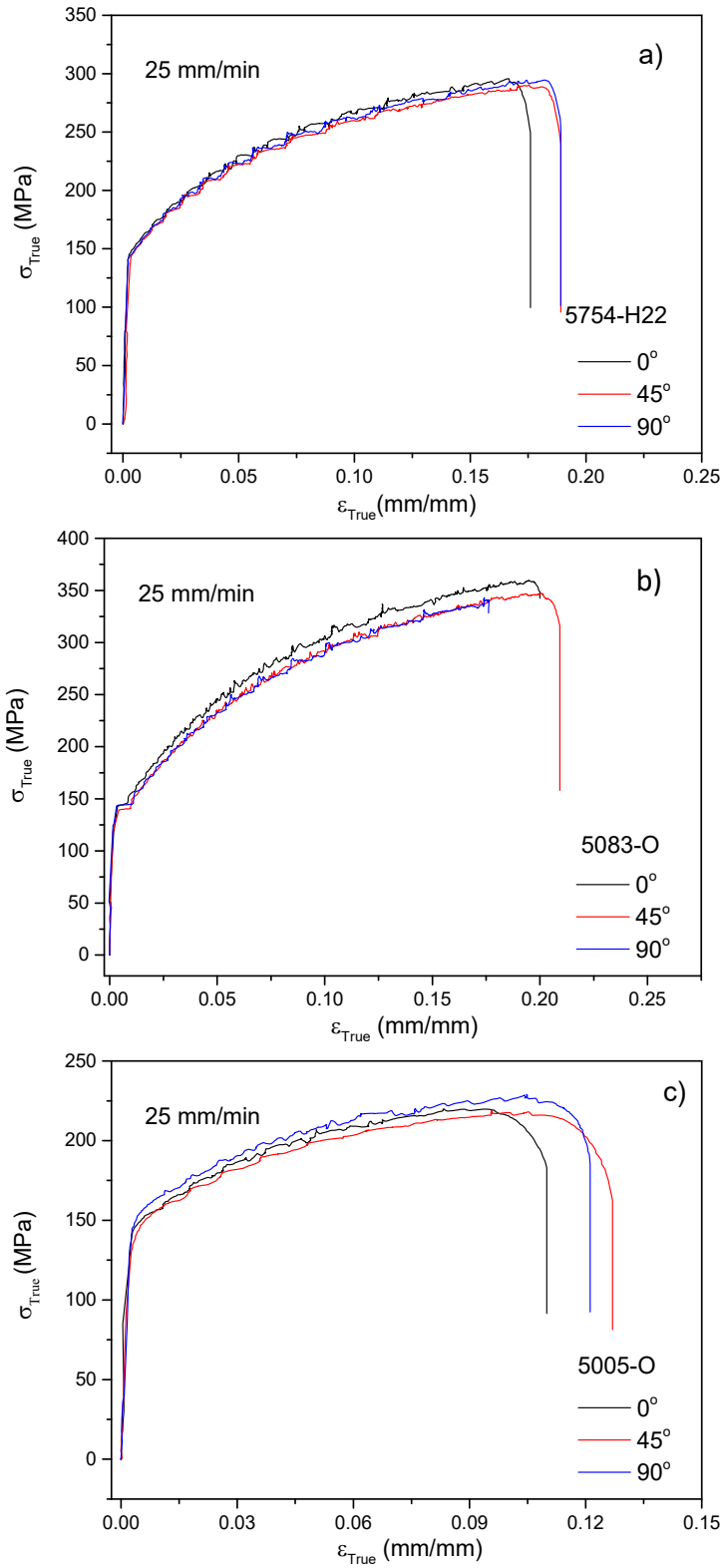


Figure 9: True stress strain curve of aluminum alloys at different orientations 5754-H22 (a), 5083- O (b) and 5005-O (c).

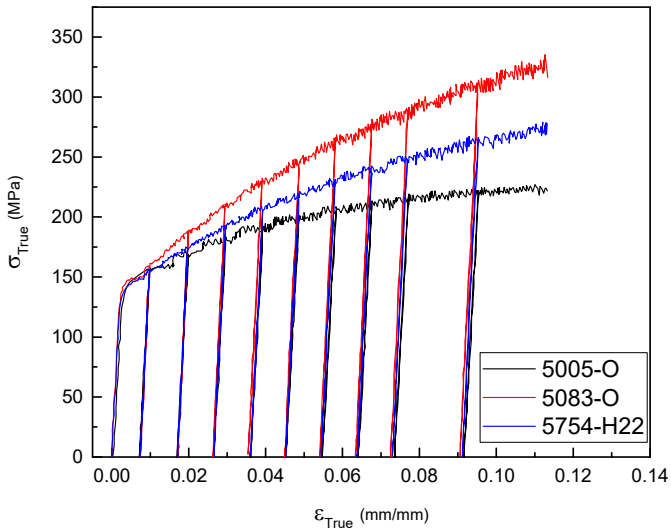


Figure 10: Load-unload stress-strain curves of the aluminum alloys at rolling direction.

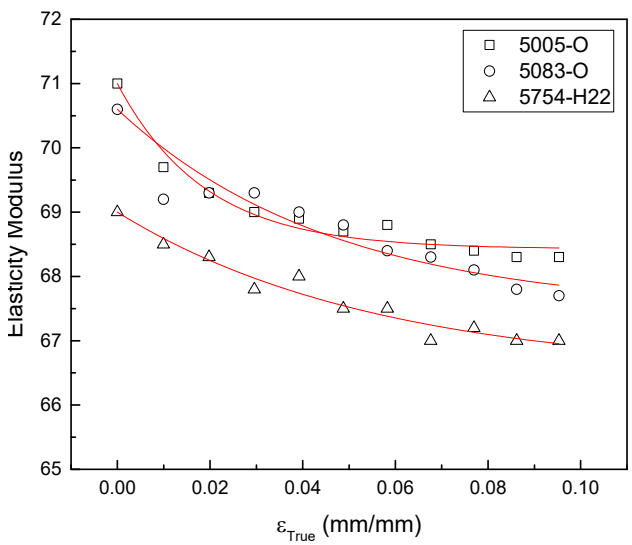


Figure 11: Variation of elastic modulus with respect to the deformation at rolling direction.

As aforementioned before, the tension-compression cyclic tests were carried out by clamping the sheet materials between the Plexiglas plates, enabling the visualization of the material inside. Therefore, it was possible to follow the marks on the samples that were used to measure the deformations by the video type extensometer. Prior to the cyclic experiments, a calibration process was performed for the video extensometers to overcome the possible errors of the marks on the samples. This type of measuring system makes possible to perform the cyclic experiments to any kind of samples that are prepared with respect to the selected standards for the small strain levels as well as the measuring the strains.

The tension-compression cyclic tests were carried out for three different strain levels and the stress-strain curves were depicted in figure 12 for the rolling direction. The strain history was chosen as $0 \rightarrow +0.01 \rightarrow -0.01 \rightarrow +0.01$. The cyclic test were also performed at 25 mm/min deformation speed.

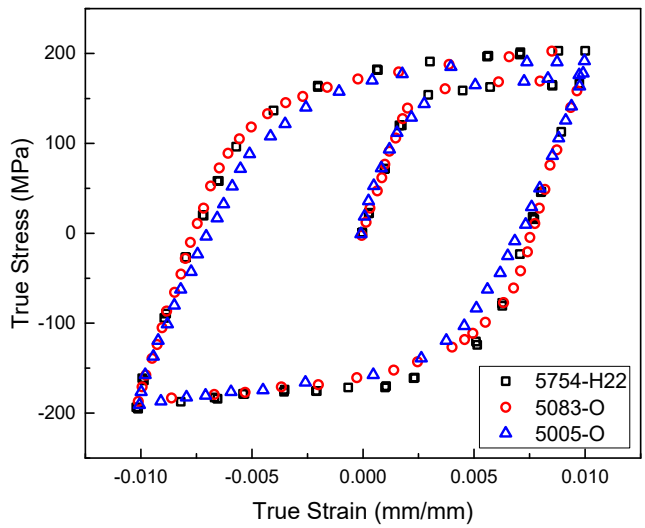


Figure 12: Experimental tension-compression cyclic behavior of the 5XXX series aluminum alloys for the rolling direction.

As can be seen from figure 12, the stress-strain curves in the obtained reverse loading conditions are very smooth for the studied materials and the Bauschinger effect is clear. Although the initial stress levels of the materials have similar magnitude, the compression strengths are different. 5005-O aluminum alloy has a higher compressive strength than the others. It is also possible to see that the stresses are the same after re-loading. The springback characterizations of the studied material were determined via the 60^{o} V-die bending test system. The test was performed to specimens at 25 mm/min deformation speed and the springback values were then measured by the bevel protractor. During these experiments, no lubrication was used and the soaking time was neglected. The measured springback angle values were 69.5^{o}, 66^{o} and 68^{o} for 5754-H22, 5083-O and 5005-O, respectively. The toleration of the springback angle error by modifying the die surfaces are required a high expertise and a very long time which affect the competition power of the sheet metal manufacturers. Therefore, the use of the finite element software increased remarkably to overcome this undesired problem. Although the performances of the commercially available software are improved by developing the used elasticity and plasticity formulations, the success on the predictions of the formability and springback are still about 75 % for the real part stamping operations. Nowadays, the optimization process are also started to be used very frequently in the simulation of the structural part designs and manufacturing processes. Particularly, the modifications of the die surfaces according to the forming and springback angle errors via the optimization processes based on the inverse engineering help the real part manufacturers. Another method suggested in this work to improve the prediction capability of the finite element software is

the determination of the model parameters used in the stamping simulations via simple experiments alone or with other classical approaches that need to be used. Therefore, in this study the Y-U model parameters were determined according to the classical approach based on the tension compression test results and both cyclic and springback test results. As the termination criteria for the optimization process, the design change tolerance and objective function tolerance were selected as 0.01 whereas the max number of the iteration was chosen as 15.

Figure 13 compares the Y-U model predictions with the experimental cyclic test results. As can be seen from the figure, the predictions show good agreement with the experiments. The model parameters are tabulated in Table 2.

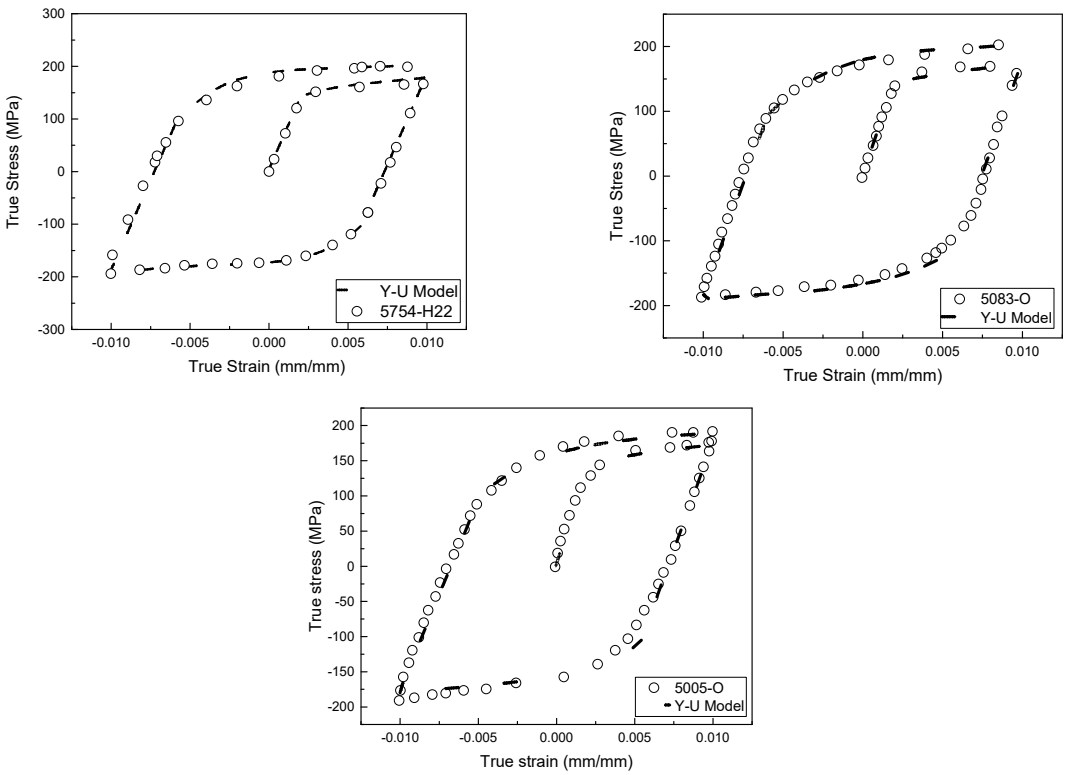


Figure 13: Y-U model predictions of the cyclic behavior of the aluminum alloys.

Materials	*Y*	*B*	*C*	R_{sat}	*k*	*b*	*m*	E_0	E_A	ξ
5754-H22	142.5	159.37	750.85	160	12.51	81.25	0.81	69	66.49	17.85
5083-O	142.75	160.15	415.42	269.55	6.28	113.44	7.94	70.6	67.46	21.52
5005-O	141.1	160.94	401.35	163.80	5.76	169.82	0.38	71	68.42	53.03

Table 2: Y-U model parameters of the specimens at rolling direction via the classical approaches.

According to the obtained parameters from the cyclic test, V-die springback simulation was run and the amounts of the springback were determined for the selected nodes that are given in figure 8. According to the simulations, the springback angle of the materials were determined as 69°, 65° and

67.2° for 5754-H22, 5083-O and 5005-O, respectively. Although the simulations are very close to the experiments, it can be improved by modifying the optimization process. As a matter of facts, these studies are going to be more valuable when the real car components are considered in the simulations due to the complexities of the deformations.

In the second case of the study, the model parameters were also determined for both cyclic stress-strain curves and springback simulations. As a target function besides the hysteresis loops of the materials, the experimental springback angle was also defined in the optimization processes. The obtained model parameters and cyclic curves are given table 3 and figure 14, respectively. In addition, the springback results for both cases are plotted in figure 15. It is seen that the differences between the model predictions and the experimental hysteresis loops are negligible for case 1 and case 2, although the springback predictions are more close to the experiments. The results show that the suitable root of the model parameters which satisfies the described targets may be different.

Materials	Y	B	C	R_{sat}	k	b	m	E_0	E_A	ξ
5754-H22	144	162.3	820	220.5	11.3	129.35	0.67	69	66.49	17.85
5083-O	145.75	165.54	625.72	282.13	6.28	135.19	9.52	70.6	67.46	21.52
5005-O	141.1	160.94	401.35	163.80	5.76	169.82	0.38	71	68.42	53.03

Table 3: The Y-U model parameters for second case.

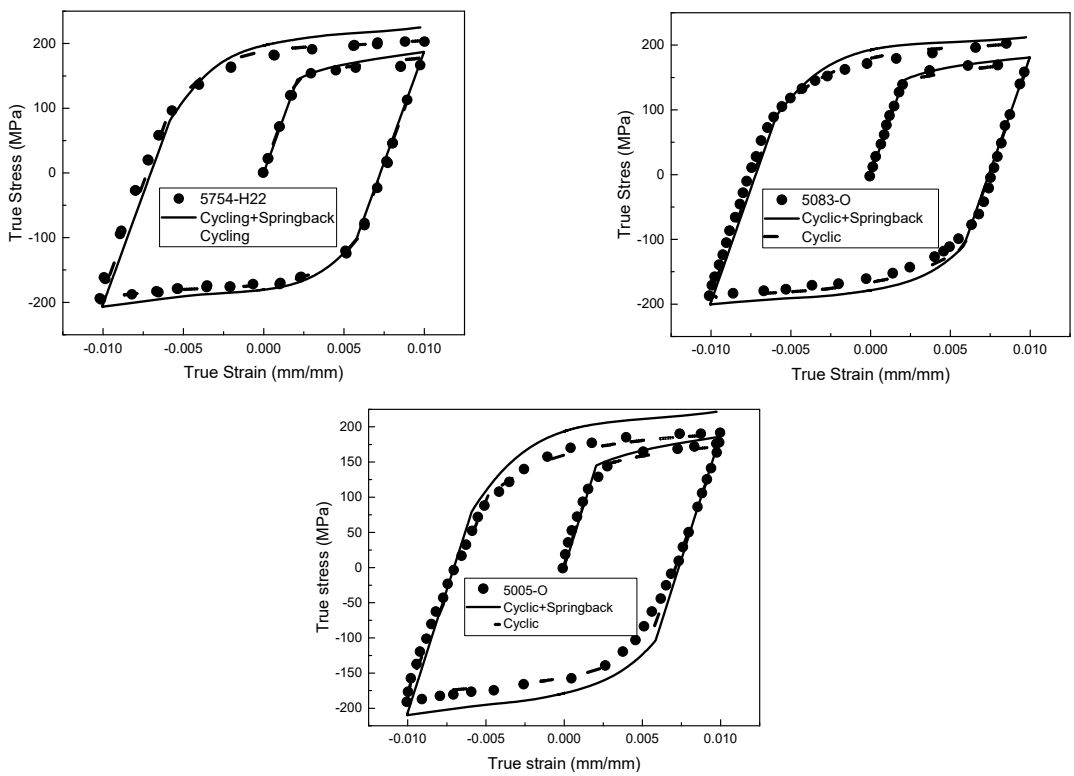


Figure 14: Comparison of Y-U model results for studied cases.

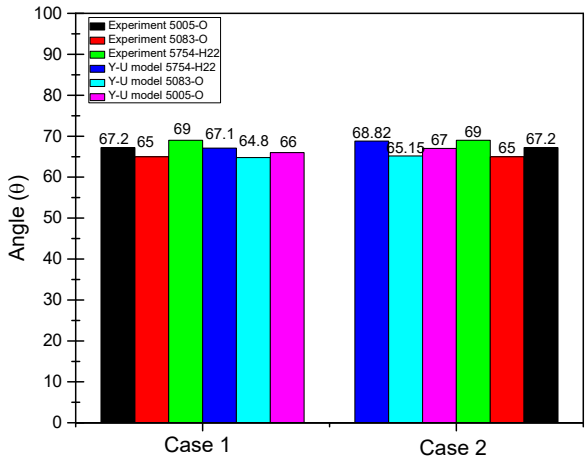


Figure 15: Comparison of V-die bending springback simulations and experimental results for studied cases.

In order to validate the new approach for the determination of the model parameters, U-bending simulations were also performed for the studied aluminum alloys. The angle between the sides of the shapes were measured and compared with the experiment in figure 16. As can be seen from the figure, the difference between the experiment and Y-U model performance which is described as Case 1 is well enough to use the cyclic test results. However, as can be seen in Case 2 the simulation results are more convenient with the experiments. Although these kinds of simple applications may not reflect the Bauschinger effect in the material, the results claim that this approach will be useful for the real applications.

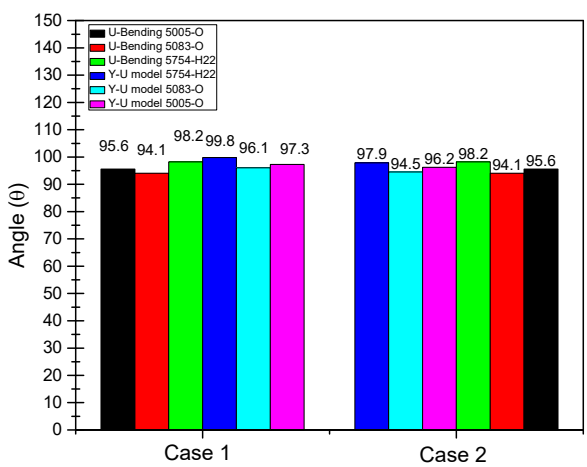


Figure 16: Comparison of U-die bending springback simulations and experimental results for studied cases.

6 CONCLUSION

In this study, the applicability of optimization process was investigated for the determination of Yoshida-Uemori two surface plasticity model parameters from cyclic stress-strain curves and

springback test results. The results revealed that the springback can be predicted more accurately when the model parameters are determined from both the definition of the hysteresis loops and springback target. Since the Yoshida-Uemori model parameters are assigned to a value of the tensile-compression stress strain hysteresis loops, we did not perform our optimizations without the cyclic test results. However, it is also possible to determine the Y-U model parameters by only considering the springback target. In addition, although there is no significant difference between the experimental and model hysteresis loops that were obtained for all cases except for 5005-O aluminum alloy, springback predictions are closer to the experimental springback results. In addition, it is aimed to use the suggested approach for a real car component to determine the new approach's performance.

References

Alghtani, A.P.C., Brooks, D.C., Barton, V.V., 2013. Springback Analysis and Optimization in Sheet Metal Forming, 9th European LS-DYNA Conference.

Aryanpour, A., Green, D.E., Evaluation of LS-DYNA, Material Models for the Analysis of Sidewall Curl in Advanced High Strength Steels, 12th European LS-DYNA Users Conference.

Boger, R.K., Wagoner, R.H., Barlat, F., Lee, M.G., Chung, K., 2005. Continuous, large strain, tension/compression testing of sheet material. Int J Plasticity 21, 2319-2343.

Chaboche, J.L., 1986. Time-Independent Constitutive Theories for Cyclic Plasticity. Int J Plasticity 2, 149-188.

Chaboche, J.L., 1989. Constitutive-Equations for Cyclic Plasticity and Cyclic Viscoplasticity. Int J Plasticity 5, 247-302.

Choi, Y., Han, C.S., Lee, J.K., Wagoner, R.H., 2006a. Modeling multi-axial deformation of planar anisotropic elasto-plastic materials, part 1: Theory. Int J Plasticity 22, 1745-1764.

Choi, Y., Han, C.S., Lee, J.K., Wagoner, R.H., 2006b. Modeling multi-axial deformation of planar anisotropic elasto-plastic materials, part II: Applications. Int J Plasticity 22, 1765-1783.

Chun, B.K., Jinn, J.T., Lee, J.K., 2002a. Modeling the Bauschinger effect for sheet metals, part I: theory. Int J Plasticity 18, 571-595.

Chun, B.K., Kim, H.Y., Lee, J.K., 2002b. Modeling the Bauschinger effect for sheet metals, part II: applications. Int J Plasticity 18, 597-616.

Dafalias, Y.F., Popov, E.P., 1975. A Model for Nonlinearly Hardening Materials for Complex Loading. Acta Mech. 21, 173–192.

Frederick, C.O., Armstrong, P.J., 2007. A mathematical representation of the multiaxial Bauschinger effect. Mater High Temp 24, 11-26.

Hill, R., 1948. A theory of the yielding and plastic flow of anisotropic metals. Proc Roy Soc London A 193, 281-297.

Hiroshi Hamasaki, Shuhei Nakamura, Vassili V. Toropov, Yoshida, F., 2011. Parameter Identification For Elasto-Plastic Constitutive Equation By Means of Cyclic Bending Experiment and Optimization, 9th World Congress on Structural and Multidisciplinary Optimization, Shizuoka, Japan.

Kessler, L., Gerlach, J., Aydin, M.S., 2008. Sipringback Simulation with Complex Hardening Materials Models, 7th LS-DYNA Anwenderforum Bamberg.

Kim, J.H., Kim, D., Lee, Y.S., Lee, M.G., Chung, K., Kim, H.Y., Wagoner, R.H., 2013. A temperature-dependent elasto-plastic constitutive model for magnesium alloy AZ31 sheets. Int J Plasticity 50, 66-93.

Lee, M.G., Kim, D., Kim, C.M., Wenner, M.L., Wagoner, R.H., Chung, K., 2005a. Spring-back evaluation of automotive sheets based on isotropic-kinematic hardening laws and non-quadratic anisotropic yield functions - Part II: characterization of material properties. Int J Plasticity 21, 883-914.

Lee, M.G., Kim, D.Y., Kim, C.M., Wenner, M.L., Chung, K., 2005b. Spring-back evaluation of automotive sheets based on isotropic-kinematic hardening laws and non-quadratic anisotropic yield functions, part III: applications. Int J Plasticity 21, 915-953.

McDowell, D.L., 1985a. A Two Surface Model for Transient Nonproportional Cyclic Plasticity—Part II: Comparison of Theory With Experiments. ASME J. Appl. Mech. 52, 303-308.

McDowell, D.L., 1985b. A Two Surface Model for Transient Nonproportional Cyclic Plasticity -Part I: Development of Appropriate Equations. ASME J. Appl. Mech 52, 298-302.

Mroz, Z., 1967. On the Description of Anisotropic Work Hardening. J. Mech. Phys. Solids 15, 163–175.

Ozturk, F., Toros, S., Pekel, H., 2009. Evaluation of tensile behaviour of 5754 aluminium-magnesium alloy at cold and warm temperatures. Mater Sci Tech-Lond 25, 919-924.

Prager, W., 1956. A New Method of Analyzing Stresses and Strains in Work Hardening Plastic Solids. ASME J. App. Mech 23, 493-496.

Stander, N., Craig, K.J., 2002. On the robustness of a simple domain reduction scheme for simulation-based optimization. Eng Computation 19, 431-450.

Thuillier, S., Manach, P.Y., 2009. Comparison of the work-hardening of metallic sheets using tensile and shear strain paths. Int J Plasticity 25, 733-751.

Tseng, N.T., Lee, G.C., 1983. Simple Plasticity Model of Two Surface Type. ASCE J. Eng. Mech. 109, 795–810.

Uemori, T., Okada, T., Yoshida, F., 1998. Simulation of springback in V-bending process by elasto-plastic finite element method with consideration of Bauschinger effect. Met Mater-Korea 4, 311-314.

Uemori, T., Okada, T., Yoshida, F., 2000. FE analysis of springback in hat-bending with consideration of initial anisotropy and the Bauschinger effect. Key Eng Mat 177-1, 497-502.

Yin, Q., Soyarslan, C., Guner, A., Brosius, A., Tekkaya, A.E., 2012. A cyclic twin bridge shear test for the identification of kinematic hardening parameters. Int J Mech Sci 59, 31-43.

Yoshida, F., Uemori, T., 2002. A model of large-strain cyclic plasticity describing the Bauschinger effect and workhardening stagnation. Int J Plasticity 18, 661-686.

Yoshida, F., Uemori, T., Fujiwara, K., 2002. Elastic-plastic behavior of steel sheets under in-plane cyclic tension-compression at large strain. Int J Plasticity 18, 633-659.

Zang, S.L., Guo, C., Thuillier, S., Lee, M.G., 2011. A model of one-surface cyclic plasticity and its application to springback prediction. Int J Mech Sci 53, 425-435.

Zeigler, H., 1959. A Modification of Prager's Hardening Rule. Q. Appl.Mech., 17, 55-65.